Adsorption (2015) 21:273–282
DOI 10.1007/s10450-015-9669-5

Molecular motion of alcohols adsorbed in ACF hydrophobic nanoslits as studied by solid-state NMR

Hiroaki Omichi[1] · Takahiro Ueda[1,2] · Taro Eguchi[1,2]

Received: 6 February 2015 / Revised: 24 March 2015 / Accepted: 30 March 2015 / Published online: 16 April 2015

Abstract The molecular motion and local structure of methanol-d_1 (CH_3OD) and ethanol-d_1 (C_2H_5OD) in activated carbon fiber (ACF) with a slit width of 0.7 and 1.1 nm have been investigated by solid-state ^1H and ^2H NMR. ^2H NMR spectra for alcohols confined in ACF gave a so-called Pake doublet below 140 K, which were characterized by the ^2H quadrupole coupling constant (QCC) of 185 kHz and the asymmetric parameter of the electric-field-gradient tensor (η) of 0.1. The QCC value of the deuteron was indicative of the hydrogen bond formation with the O···O distance of ca. 0.27 nm, suggesting the solid-like feature of alcohols in ACFs. The quadrupole broadening vanished on heating and the single isotropic resonance line was observed. Alcohol molecules were undergoing a rapid motion like as in the bulk liquid, indicating a transition from solid to liquid in ACFs. Temperature-dependent ^1H NMR spectra were used for evaluating the E_a value for reorientation in solid-like alcohols, whereas the ^2H NMR spectra were used for obtaining the translation accompanying reorientation in liquid-like alcohols. Alcohols with a bilayered structure in ACF with a slit width of 1.1 nm gave similar E_a values, whereas C_2H_5OD in ACF with a slit width of 0.7 nm, in which a monolayered structure is expected, exhibited a cross-over of two activation processes at 172 K. The variation in E_a was probably caused by the structural relaxation concerning with the hydrogen bonding formation and/or excitation of the large amplitude local motion. The competition of the directionality of hydrogen bonds and a freedom of molecular orientation plays an important role to characterize the intermolecular structure as well as the physicochemical properties in amphipathic molecules in confinement.

Keywords Molecular motion · NMR · 2D porous materials · Amphipathic molecular system · Confinement · Hydrogen bond

1 Introduction

Dimensionality of nanospace evokes noteworthy and peculiar effects on the intermolecular structure and the physicochemical properties of the confined molecules. In particular, the two-dimensional system is an ideal model for examining the effect of the anisotropic intermolecular interactions on the cooperative phenomenon such as phase transition. Activated carbon fiber (ACF) consists of amorphous carbon but includes micrographites (nanometer-sized graphenes). The interstices of the micrographites provide uniform and slit-type micropores (Kaneko et al. 1992; Oshida et al. 1995; Sato et al. 1997), leading to large micropore volume and super-high specific surface area. Thus, the nanoslit in ACF is regarded as a pseudo-two-dimensional and hydrophobic nanospace, and will serve the unique and anisotropic potential field reflecting the dimensionality.

Such a quasi-two-dimensional space will give rise to a specific state of molecular condensation. X-ray diffraction,

Electronic supplementary material The online version of this article (doi:10.1007/s10450-015-9669-5) contains supplementary material, which is available to authorized users.

✉ Takahiro Ueda
ueda@museum.osaka-u.ac.jp

[1] Department of Chemistry, Graduate School of Science, Osaka University, Toyonaka, Osaka 560-0043, Japan

[2] The Museum of Osaka University, Osaka University, Toyonaka, Osaka 560-0043, Japan

small-angle X-ray scattering, and GCMC simulation studies have succeeded in clarifying the average local structures of the confined molecules in ACF micropores (Kaneko 1996; Mowla et al. 2003; Śliwińska-Bartkowiak et al. 2012; Nguyen and Bhatia 2011). Regarding the physicochemical properties of the condensed matter confined in ACFs, the global phase diagram including the specific phases that appeared in ACF was proposed by Radhakrishnan et al. (2000, 2002a). Importantly, the melting point elevation of the condensed phase in ACF is quite interesting, which was found for several guest compounds such as C_6H_6 (Watanabe et al. 1999), CCl_4 (Kaneko et al. 1999; Radhakrishnan et al. 1999), aniline (Radhakrishnan et al. 2002b), and methanol (Śliwińska-Bartkowiak et al. 2001). This phenomenon is unique because it lacked a melting point depression observed in mesopores. Furthermore, an intermediate liquid crystalline phase was known to appear between solid and liquid phases. This liquid crystal phase is called "hexatic phase", in which molecules form sixfold orientational order, but not long-range positional ordering. Evidence for an intrinsic hexatic phase was observed in some 2-D systems (Radhakrishnan et al. 2000, 2002a). Indeed, we recently found the specific behavior of molecules confined in ACF from the viewpoint of molecular motion; 2D melting of $CDCl_3$ (Ueda et al. 2010a) and the impurity effect of trace amounts of $CHCl_3$ on 2D melting for CCl_4 (Ueda et al. 2010b).

In the nanospace with the hydrophobic characters, dispersion forces and hydrogen bonding are remarkable and dominate intermolecular interactions, which control both the intermolecular structure and the physicochemical properties. The former is important for hydrophobic molecules such as $CHCl_3$ (Ueda et al. 2010a), CCl_4 (Ueda et al. 2010b), and adamantane (Omichi et al. 2008), and affect the confined molecules mainly through the guest–wall interactions. The latter is significant for hydrophilic molecules such as $H(D)_2O$ in ACF (Omichi et al. 2007; Ohba et al. 2004a, b, 2005), and will affect the confined molecules through guest–guest interactions by hydrogen bonding. Thus, from the viewpoints of intermolecular interactions, the amphipathic molecules such as alcohols are very curious, because it is expected that a competition between the hydrophobic and hydrophilic interactions will trigger the specific physicochemical properties of alcohols. Methanol (CH_3OH) and ethanol (C_2H_5OH) are well-known, the most ubiquitous, and the simplest amphipathic molecules. In bulk methanol, there are two crystal polymorphism, both of which have orthorhombic structure ($P2_12_12_1$ for α phase and *Cmcm* for β phase), and the melting point of the β phase is 175.4 K (Torrie et al. 2002). On the other hand, bulk ethanol shows the further complex polymorphism (Ramos et al. 2006); four crystalline phases (α, β, γ, δ) and two disordered phases [ordinary glass (amorphous) and orientationally-disordered crystal (glassy crystal)]. The melting point is 159 K. These phases appear depending on the thermal histry (rasing or cooling rate, annealing temperature and so on). The confinement effect on the crystal polymorphism for alcohols is also interesting. For example, freezing behaviour of methanol confined in ACF ($w = 1.8$ nm) was studied by dielectric spectroscopy (Śliwińska-Bartkowiak et al. 2001), and three thermal anomalies was found; 157 K for α–β transition similar to that in the bulk crystal, 218 K for crystal-hexatic transition which is specified in 2D system, and 256 K for hexatic-liquid transition. X-ray diffraction study revealed that ethanol confined in mesoporous silicon (10 nm of diameter and 50 μm of length) showed the similar polymorphism to bulk one at higher filling factor ($f > 0.71$), whereas the adsorbed film corresponding to three monolayer thick ($f < 0.41$) remains in an amorphous state from 80 to 150 K (Henschel et al. 2010).

In fact, the structures of methanol and ethanol in ACF have also been investigated by diffraction methods (Ohkubo et al. 1999a, b, 2000, 2001; Iiyama et al. 2009). Alcohol molecules confined in the hydrophobic nanospace form a solid-like structure with a position-order of molecules even at 303 K. In particular, ethanol molecules also have an orientational order, which brings about the oriented molecular arrangement of ethanol parallel to the pore walls. Recently, a calorimetric study was conducted for the alcohol adsorption onto ACF (Nobusawa et al. 2013), and has pointed to the important role of the surface carbonyl groups on the differential heat as well as isotherms for alcohol adsorption. However, the dynamic aspects of the confined molecules have not yet been clarified in ACF. The dynamic features of guest molecules will make it possible to examine the properties of condensed phases in the ACF nanospace based on the guest–wall and guest–guest interactions.

NMR spectroscopy is a useful tool to detect microscopic information around the probe nuclei, and yields information about the dynamic and local structures of molecules containing the probe nuclei. Deuterized alcohols (CH_3OD and C_2H_5OD) enable us to investigate molecular motion through alkyl and hydroxyl groups, respectively. In this work, solid-state ^1H and ^2H NMR spectra were measured on CH_3OD and C_2H_5OD confined in ACFs. Herein, we discuss the local structure as well as the dynamic aspects of alcohols in ACFs.

2 Experimental

Pitch-based ACFs with different pore widths were supplied by Osaka Gas Co. Ltd., which are denoted as ACF10A and ACF20A, respectively. The characterization of the ACF

micropores was carried out in our previous work by the N_2 adsorption isotherm, and the results were presented elsewhere (Ueda et al. 2006). The slit width of ACFs was 0.7 nm for 10A and 1.1 nm for 20A.

The powdered ACF 10A and 20A samples were evacuated at room temperature for 1 day under reduced pressure (10^{-2} Torr), and then at 437 K for 2 h. The pretreated ACF powders were explored under CH_3OD vapour at room temperature for 2 days using a vacuum line for loading guest molecules, whereas the appropriate amount of C_2H_5OD (90 % of a pore volume) was added to the pretreated ACF powders by micro syringe under N_2 atmosphere. Anhydrous CH_3OD and C_2H_5OD (D 99 at.%) were purchased from Wako Pure Chemical Industries, Ltd. and were handled under a N_2 atmosphere. The prepared specimens were sealed into glass ampoules (5 mm ϕ) with He gas (ca. 200 Torr).

All NMR measurements were conducted using a spectrometer (DSX-200; Bruker Analytik GmbH) equipped with superconducting magnet (4.7 T), which is operating at the Larmor frequency of 200.13 MHz for ^1H and 30.7 MHz for ^2H nuclei. The free induction decay (FID) signals were recorded using the appropriate pulse sequences: a single pulse rf excitation was used for ^1H spectra (4–5 μs length of π/2-pulse), whereas the single pulse as well as the solid-echo pulse sequence (π/2–τ–π/2–τ–acqu.) was used for ^2H spectra (3–3.5 μs length of π/2-pulse and a 20 μs pulse interval). Temperature control was achieved by flowing N_2 gas, which was regulated within the experimental error of ±1 K using a temperature controller (VT-3000; Bruker Analytik GmbH). The temperature of samples was monitored with a Cupper–Constantan thermocouple (T-type) thermometer.

3 Results and discussion

At first, we examined ^2H NMR for alcohols confined in ACFs. Both alcohols gave rise to the broad and structural line shapes with the quadrupole broadening below 140 K. Figure 1 shows the typical examples of the line shape, which are so-called Pake doublet powder patterns characterized by the ^2H quadrupole coupling constant (QCC; e^2qQ/h) of 185 kHz and the asymmetric parameter of the electric-field-gradient tensor (η) of 0.1 for both CH_3OD and C_2H_5OD. In fact, it is well known that the QCC value for the deuteron in O–D···O type hydrogen bonds is in good correlation with reported O···O distances (Olympia and Fung 1969; Berglund and Vaughan 1980). The evaluated QCC value (185 kHz) gives the O···O distance of ca. 0.27 nm, which agrees with the O···O distance (0.2716 and 0.2730 nm) for crystal phase I in the bulk ethanol crystal (Jönsson 1976). This strongly suggests that each of CH_3OD and C_2H_5OD is a solid and forms intermolecular hydrogen bonds in ACFs.

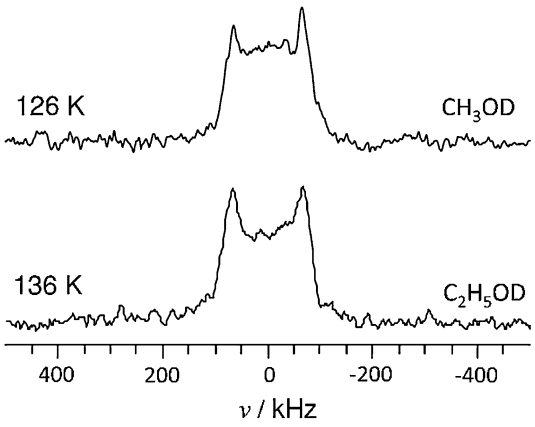

Fig. 1 ^2H NMR spectra for alcohol confined in ACF20A; CH_3OD and C_2H_5OD

The powder spectrum collapsed by activation of the local motion of the OD-group on heating, and the quadrupole broadening vanished above the following temperatures: 158 K in 10A and 138 K in 20A for CH_3OD, and 180 K in 10A and 156 K in 20A for C_2H_5OD. On further heating, an isotropic resonance line was observed above the following temperatures: 160 K in 10A and 140 K in 20A for CH_3OD, and 200 K in 10A and 170 K in 20A for C_2H_5OD. In the temperature region where no signal was observed, the ^2H NMR spectrum reaches the maximum broadening where the frequency of the molecular motion becomes same order to the quadrupole interaction. Figure 2 shows the temperature dependence of the isotropic resonance lines. The complete averaging of the ^2H quadrupole interaction strongly suggests the rapid isotropic reorientation and translation of alcohols as in the bulk liquid, implying a transition from solid to liquid in ACFs. Figure 3 depicted the temperature dependence of the line width (FWHM) for the isotropic peak. Narrowing of the line width on heating indicates that the rate of molecular motion is in the extreme narrowing region. Since the narrowing in the case of ^2H nuclei is caused by the orientational fluctuation of the principal axis component of the quadrupole coupling tensor, the translation accompanying the change in the molecular orientation will also achieve the effective narrowing of the resonance line, in addition to the isotropic reorientation. The line width obeys the Arrhenius' law in the low temperature region, indicating that the thermal motions such as translation and isotropic reorientation take place. However, the slope changes around 210–220 K. This will be mainly dominated by the inhomogeneity of the external field as well as the bulk susceptibility of the ACF powdered samples.

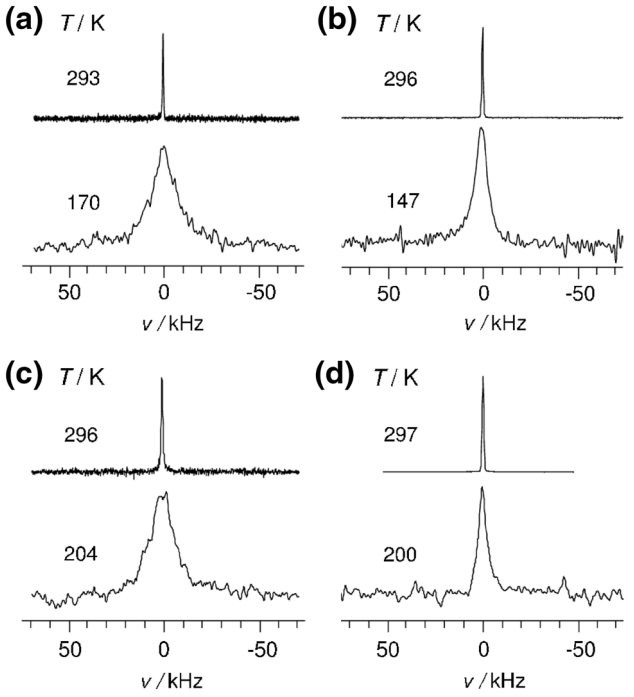

Fig. 2 ^{2}H NMR spectra for alcohol confined in ACF; CH_3OD in ACF 10A (**a**) and 20A (**b**) and C_2H_5OD in ACF 10A (**c**) and 20A (**d**)

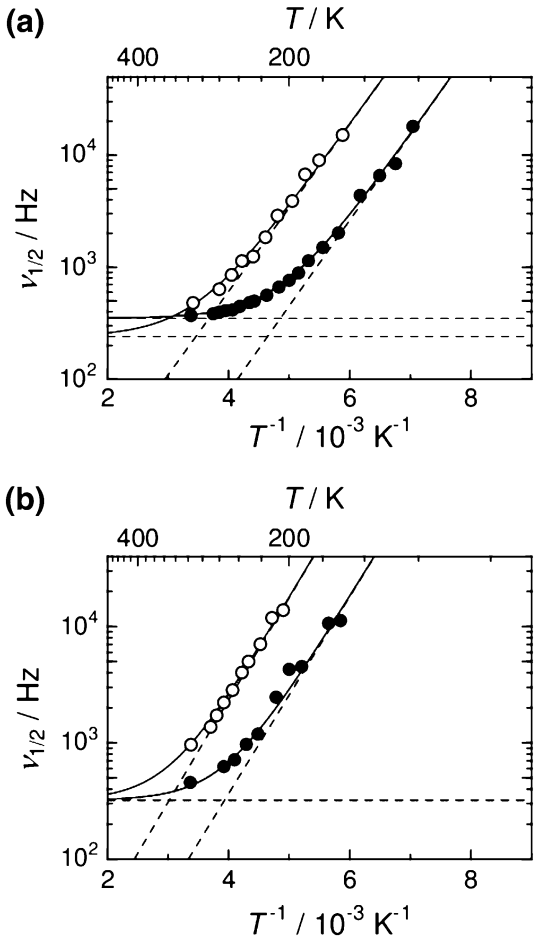

Fig. 3 Arrhenius plot of the line width of ^{2}H NMR of alcohols confined in ACF 10A (*open circle*) and 20A (*filled circle*); CH_3OD (**a**) and C_2H_5OD (**b**)

In the case of ^{1}H spectra, the ^{1}H–^{1}H magnetic dipolar interaction mainly contributes to the line width of alcohols. The translation as well as the isotropic reorientation of alcohols plays an important role in narrowing the line width, because the dipolar interaction is presented as a function of both the internuclear distance and orientation of ^{1}H–^{1}H vector with respect to the external magnetic field. Therefore, it is expected that the temperature dependence of the ^{1}H line width provides the dynamic aspect of alcohols concerning translational diffusion and isotropic reorientation.

Figure 4 shows the temperature dependence of the ^{1}H spectra. Both alcohols gave an isotropic resonance line in the temperature range from 130 K to room temperature, and the line width strongly depended on the temperature. In C_2H_5OD, the full width at half maximum (FWHM) at room temperature is ca. 800 Hz (4 ppm), which is much greater than the chemical shift separation of ca. 1 ppm between methyl and methylene protons as well as the line width in bulk liquid (See Supplementary Information). The line width broadens to be 15 kHz in ACF10A and 12 kHz in ACF20A at 130 K. The temperature dependence suggests vigorous molecular motion (translation and/or isotropic reorientation) just like the liquid state for C_2H_5OD in ACF, but the rate of the motion is slower than those in bulk liquid. The observed spectra for CH_3OD in ACF also behave in the same manner as those for C_2H_5OD, although the line width was somewhat narrow. The ^{1}H spectra for alcohols in ACF are quite different from the bulk one, which is provided in Supplementary Information.

Figure 5 depicts the temperature dependence of the line width (FWHM) for the ^{1}H resonance line. In the temperature range above 180 K for CH_3OD and above 210 K for C_2H_5OD, the line width depends less on temperature, which will mainly be dominated by the inhomogeneity of the external field as well as the bulk susceptibility of the ACF powdered samples. In the spectra for bulk alcohols, inhomogeneity of the external field is estimated to be less than 250 Hz (See Supplementary Information). Therefore, the temperature-independent intrinsic line width is caused by the bulk susceptibility of the ACF powdered samples. In contrast, below these temperatures, the line width increases according to Arrhenius' law, where the thermally activated molecular motion substantially affects the resonance line. The observed broadening upon cooling indicates a slowing down of molecular motion. According to Garg and Davidson, a FWHM of 21 kHz was reported for the ^{1}H wide-line NMR spectrum in bulk CH_3OD crystal between

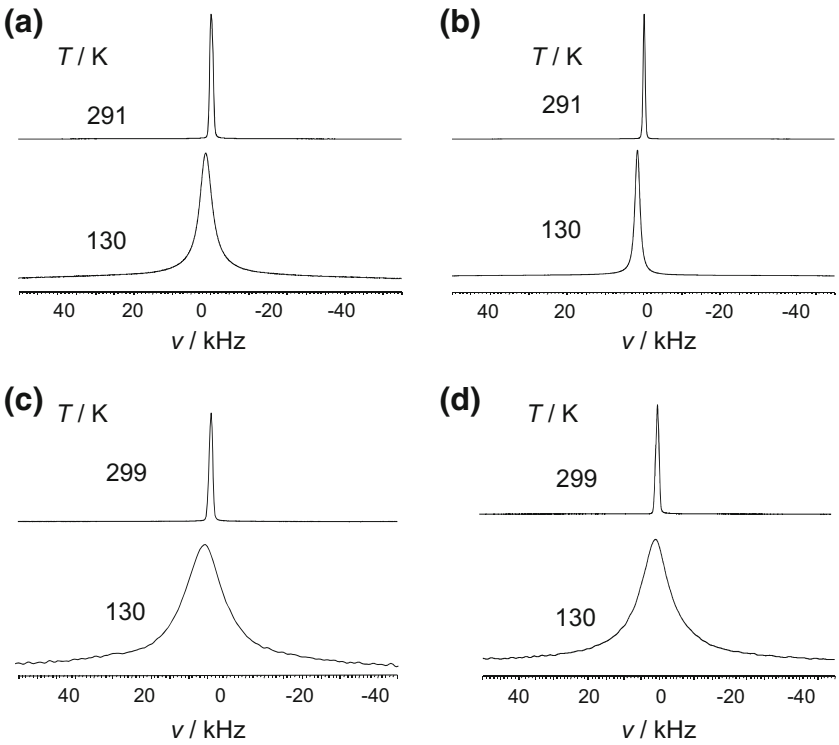

Fig. 4 ^{1}H NMR spectra for alcohol confined in ACF; CH_3OD in ACF 10A (**a**) and 20A (**b**) and C_2H_5OD in ACF 10A (**c**) and 20A (**d**)

4.2 and 160 K (Garg and Davidson 1973). The second moment of ^{1}H spectrum for CH_3OD with rotating CH_3 groups was also evaluated to be 5.56 G^2 as the intramolecular contribution (Garg and Davidson 1973), which corresponds to FWHM of 23 kHz for a Gaussian line shape. Furthermore, Eguchi et al. also reported the second moment of ^{1}H NMR spectra for solid ethanol to be 14 G^2 at the melting point (159.0 K) of the stable and ordered phase with monoclinic lattice (crystal I) (Eguchi et al. 1980). This second moment value corresponds to the FWHM of 35 kHz for the Gaussian line shape.

The observed line widths of both CH_3OD and C_2H_5OD in ACF are much narrower than those in bulk solid, strongly suggesting that alcohols are undergoing the rapid isotropic molecular motion in ACFs. For CH_3OD in both 10A and 20A, the thermal anomalies, which have been reported by dielectric study (Śliwińska-Bartkowiak et al. 2001), were not observed in the temperature dependence of the ^{1}H and ^{2}H line widths. This may be concerned with the difference in the pore width: The pore width in our study ($w = 0.7$ and 1.1 nm) is narrower than that in the previous study ($w = 1.8$ nm). In the case of ^{1}H spectra, there are some motional modes to reduce the dipolar interactions including the overall molecular reorientation, translational diffusion, local motion of alkyl-groups, and so on. Since the methyl rotation has already done the reduction of the dipole–dipole interaction below 130 K (Garg and Davidson 1973), the residual dipolar interaction would be averaged out by the overall molecular reorientation, translational diffusion and the large amplitude local motion such as kink, twisting, and reorientation of alkyl-group, except for methyl rotation. Such motions will mainly average the dipolar interaction for methylene protons. However, the ^{2}H NMR experiments support solid-like alcohols in ACFs below 158 K in 10A and 138 K in 20A for CH_3OD, and below 180 K in 10A and 156 K in 20A for C_2H_5OD, as described above. The remarkable narrowing of the ^{1}H NMR spectrum was observed even below these temperatures, where translation of the alcohol molecule is frozen. Therefore, it is valid that the ^{1}H line widths are mainly modulated by the isotropic reorientation of alcohols as well as the large amplitude local motion of alkyl-group except for methyl rotation.

Thus, our solid-state NMR study reveals a dynamically disordered structure of alcohol molecules with high mobility like a liquid state at ambient temperature. This dynamic structural feature of alcohol molecules seems to be inconsistent with a positional and orientational ordered structure of alcohol molecules (Ohkubo et al. 1999a, b, 2000, 2001; Iiyama et al. 2009). However, the difference in these structural features will be explained by the observation timescale. That is, alcohol molecules are dynamically disordered in the NMR time scale, but form the positional and/or orientational ordered structure as a time and ensemble average.

The analyses of the temperature-dependent line width give rise to the activation energy of molecular motion, which includes the knowledge of the intermolecular

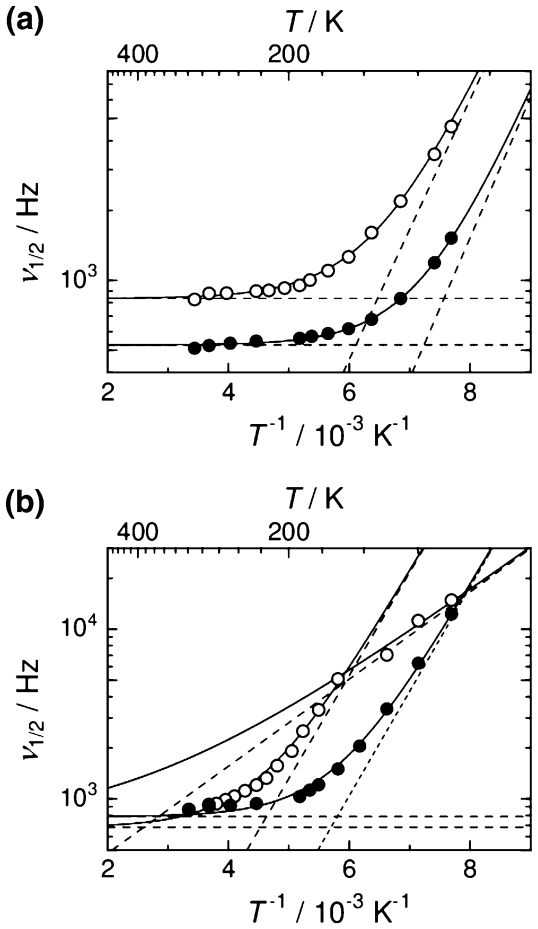

Fig. 5 Arrhenius plot of the line width of ^{1}H NMR of alcohols confined in ACF 10A (*open circle*) and 20A (*filled circle*); CH_3OD (**a**) and C_2H_5OD (**b**)

interactions. The line width of the isotropic peak can be represented by assuming superposition between the temperature-independent ($\nu^0_{1/2}$) and the temperature-dependent [$\nu_{1/2}(T)$] components. The former is the intrinsic line width stemming from the inhomogeneity of the magnetic field, and the latter corresponds to the motional narrowing part which is proportional to the spin–spin relaxation rate ($1/T_2$) in the extreme narrowing region (Abragam 1961). Furthermore, $1/T_2$ is proportional to the square of the nuclear spin interaction (C_i, $i = Q$ and D for quadrupole and dipole interactions, respectively) and the correlation time (τ_c), of which temperature dependence follows the Arrhenius' law:

$$\nu_{obs} = \nu^0_{1/2} + \nu_{1/2}(T) \quad (1)$$

$$\nu_{1/2}(T) = 1/\pi T_2 = C_i^2 \cdot \tau_c, \quad (2)$$

$$\tau_c = \tau_0 \exp(E_a/RT), \quad (3)$$

where $C_Q = \sqrt{3/8}(2\pi)(e^2qQ/h)$ and $C_D = \sqrt{3/2}(2\pi)(\gamma^2 h/r^3)$. Using the QCC (185 kHz) and the typical dipolar interaction (for example, 21 kHz for methylene protons with $r_{H-H} = 1.79$ Å), the resultant τ_c value from ^{1}H resonance line is 20 times longer than that from ^{2}H resonance line, when ^{1}H and ^{2}H spectra have same linewidth. That is, the molecular motion detectable for ^{1}H resonance line is slower than that for ^{2}H resonance line. According to these relations, the line widths of ^{2}H resonance line in Fig. 3 correspond to the correlation time from 2.5×10^{-9} to 1.2×10^{-7} s, whereas those of ^{1}H resonance line in Fig. 5 correspond to the correlation time from 6.0×10^{-8} to 2.4×10^{-6} s.

The slope provides the apparent activation energy (E_a) for the molecular motion of alcohols. The ^{1}H NMR spectra yield the E_a values for isotropic reorientation in the solid-like alcohol in ACFs, whereas the ^{2}H NMR spectra are concerned with the average E_a values for translation accompanying the orientational change as well as the isotropic overall reorientation in the liquid-like alcohol. The resultant E_a values are listed in Table 1. For C_2H_5OD in 10A, two activation processes are postulated, because the temperature dependence of the ^{1}H line width shows the inflection point at 172 K as shown in Fig. 5b. The possibilities for the origin of the two activation processes will be mentioned below.

In general, breaking the hydrogen bond mainly corresponds to the activation process for molecular reorientation

Table 1 Apparent activation energy of alcohols confined in ACFs

System	Method	E_a (kJ mol^{-1})	Motional mode
ACF10A			
CH_3OD	$\nu_{1/2}(^1H)$	11	Reorientation
	$\nu_{1/2}(^2H)$	14	Translation and reorientation
C_2H_5OD	$\nu_{1/2}(^1H)$	9 (<172 K)	Reorientation
		12 (>172 K)	
	$\nu_{1/2}(^2H)$	17	Translation and reorientation
ACF20A			
CH_3OD	$\nu_{1/2}(^1H)$	12	Reorientation
	$\nu_{1/2}(^2H)$	14	Translation and reorientation
C_2H_5OD	$\nu_{1/2}(^1H)$	12	Reorientation
	$\nu_{1/2}(^2H)$	16	Translation and reorientation
Bulk liquid			
CH_3OD[a]	^{2}H-NMR	11.5	Reorientation
CH_3OH[b]	Flow	12.9 ± 0.3	Self-diffusion
C_2H_5OD[a]	^{2}H-NMR	18.4	Reorientation
C_2H_5OH[b]	Flow	19.0 ± 0.7	Self-diffusion

[a] Goldammer and Hertz (1970)

[b] Pratt and Wakeham (1977)

of alcohols, whereas the defect formation and rearrangement of the surrounding molecules accompanies molecular translation. In bulk liquids, both motional modes are coupled each other, leading to comparable E_a values for molecular reorientation and self-diffusion. On the other hand, the E_a values for translation are somewhat larger than those for reorientation in ACFs. This feature supports that the ^{2}H NMR spectra focus on the dynamic behavior of liquid-like alcohols in ACF, whereas the ^{1}H NMR spectra attract those of solid-like alcohols. Furthermore, the E_a values in both alcohols seem to depend less on the slit width, except for C_2H_5OD in 10A, implying similar environments and intermolecular interactions for alcohol molecules in ACF10A and 20A. That is, the potential barrier for the molecular motion of alcohols is dominated by the special restriction due to the slit-type nanospace (hydrophobic character) as well as the intermolecular hydrogen bond (hydrophilic character). However, for C_2H_5OD in 10A, the cross-over of the activation processes has been observed, indicating the existence of any transitions which accompanies the change in the intermolecular interactions.

At this point, the presumable intermolecular structures of alcohols in ACF are envisaged by the potential profiles through the molecular size relative to the ACF nanospace. For infinite slit pores composed of the graphite sheets with the separation of H, the equilibrium position of the globular guest molecules will be predicted by the well-known Steele's 10-4-3 potential $U(z)$ (Steele 1973).

$$U(z) = (2\pi\rho_s\varepsilon_{sf}\sigma_{sf}^2\Delta)\left[\frac{2}{5}\left(\frac{\sigma_{sf}}{z}\right)^{10} - \left(\frac{\sigma_{sf}}{z}\right)^{4} - \frac{\sigma_{sf}^4}{3\Delta(0.61\Delta + z)^3}\right] \quad (4)$$

where ρ_s is the number density of the solid wall (114 nm^{-3} for graphite), and the subscript s and f represent the surface and the fluid, Δ is the distance between lattice planes, z is the coordination of a fluid molecule along the direction perpendicular to the surface plane, ε_{sf} and σ_{sf} are the cross interaction parameters between the fluid and the surface. Here, σ_{sf} is generally estimated by the Lorentz–Berthelot rule as $\sigma_{sf} = 0.5\ (\sigma_{ss} + \sigma_{ff})$. For alcohols, the σ_{ff} values are approximated by the rough hard-sphere diameter; 0.365 nm for CH_3OH and 0.424 nm for C_2H_5OH (Hurle et al. 1985). For graphite, 0.34 nm was used as σ_{ss}. The total potential energy for the confined molecule in the slit pore is represented by the sum of the potential energy from both sides of the slit wall as follows (Kaneko 1996):

$$\Phi(z, H) = U(z + H/2) + U(z - H/2). \quad (5)$$

In this case, the origin of the coordination for the variable z is the centre of the slit pore, satisfying the condition; $-H/2 < z < H/2$. According to Eqs. 4 and 5, the shape of the potential profile critically depends on the relative size between the slit width and the confined molecule: For $H/\sigma_{sf} > 2.25$, a double-minimum potential begins to develop with a hump at the centre of the slit. The effective pore width, w, determined from adsorption experiments is related to H as $H = w + 0.8506\sigma_{ss} - \sigma_{ff}$ (Kaneko et al. 1994). The H/σ_{sf} value is then evaluated to be 1.81 in 10A and 2.94 in 20A for CH_3OD and to be 1.57 in 10A and 2.62 in 20A for C_2H_5OD.

The double minimum potential profile is expected for 20A. This potential profile is amenable to a bilayer structure for alcohols in 20A, resulting in the similar intermolecular structure and the dynamic behaviour of CH_3OD and C_2H_5OD in ACF20A. This structural feature for CH_3OD and C_2H_5OD in ACF is also supported by diffraction studies. Ohkubo and co-workers have also suggested the bilayer packing and solid-like ordered structures of CH_3OH and C_2H_5OH in ACF with the slit width of 1.1 nm as an average structure (Ohkubo et al. 1999a, b, 2000, 2001). In contrast, the single minimum potential profile is expected for 10A, where the monolayer structure of alcohol molecules is preferable in 10A. The narrow slit in 10A enforces the guest–guest as well as the guest–wall interactions, eliciting the solid-like feature of the confined alcohols. According to Ohkubo et al. (1999b), C_2H_5OH molecules form a positional and orientational ordered structure in ACF. In contrast, CH_3OH molecules form a positional ordered structure, but not orientational ordering. The CH_3OH molecules in ACF have more freedom of rotational motion than C_2H_5OH. The dynamics of alcohols in 10A is also consistent with these structural features: CH_3OD shows the high mobility for isotropic reorientation and translation, whereas C_2H_5OD shows the cross-over of two activation processes.

The monolayer structure of alcohols in 10A is expected to enhance two-dimensionality in the intermolecular interaction between alcohol molecules. In particular, for C_2H_5OD, the two-dimensionality in the intermolecular interactions is enhanced more effectively than CH_3OD, because both the spatial restriction and enforcing of the intermolecular interaction are more remarkable for the large molecule. Intensifying the two-dimensionality in the intermolecular interactions will reflect on the orientational ordering of alcohols as well as physicochemical properties. In the case of C_2H_5OD, the hydrogen bond plays an important role in the dynamic behavior as well as the formation of monolayer structures in ACF. In the bulk solvent, C_2H_5OH exhibits polymorphism such as a fully ordered (monoclinic) crystal, a (bcc) plastic crystal, orientationally disordered crystal (glassy crystal), and ordinary amorphous glass (Ramos et al. 2006). In a fully ordered (monoclinic) crystal, C_2H_5OH molecules form a zig-zag hydrogen bonding chain (Jönsson 1976). Such

hydrogen bonding chain has been observed in C_2H_5OH monolayer adsorbed on the graphite surface (Morishige 1992). On the other hand, the orientational disorder causes the plastic crystal and ordinary amorphous glass. Thus, the competition of the degree-of-freedom of molecular orientation and the directionality of hydrogen bonding critically dominates the properties of the condensed phase. In the bilayer structure in ACF, C_2H_5OD molecules can form pseudo-3-dimensional hydrogen bonds along the in-plane and interlayer directions. However, in the monolayer structure, the formation of hydrogen bonds is restricted to the 2-dimensional in-plane direction. In fact, the melting points of 2D C_2H_5OH crystal (204–214 K), which depend on the coverage, were much higher than bulk one (159 K) (Morishige 1992). The confinement into 2-dimensional space and monolayer structure of C_2H_5OD in 10A may feasibly proceed the the 2D crystal formation of C_2H_5OD similar to monolayer adsorbed on graphites. Thus, the liquid-2D crystal transition is one of the possibilities for the inflection point at 172 K in Fig. 5b. In this case, the cross-over corresponds to the transition from isotropic molecular reorientation to the local motion of alkyl-group, because the translational and orientational motion of C_2H_5OD freezes by development of the hydrogen bonding network in the 2D crystal. In contrast, XRD study has revealed that ethanol adsorbed on the pore wall of the mesoporous silicon, of which thickness corresponds to three monolayer, remains in an amorphous state from 80 to 150 K (Henschel et al. 2010). Thus, the anisotropic spatial environment facilitates a failure of the development of a hydrogen bond network. As a result, the defect formation of the hydrogen bond proceeds and the contribution of hydrogen bonding to the intermolecular interaction is reduced. According to this scenario, C_2H_5OD in ACF10A below 172 K may be in the orientationally disordered solid like a hexatic phase, glassy crystal or ordinary amorphous glass, where C_2H_5OD molecules make it possible to undergo the over-all reorientation under the lower potential barrier.

Form the viewpoints of the molecular motion, we proposed two possibilities for the bending observed in the Arrhenius plot in Fig. 5b: the liquid-2D crystal transition and the liquid-amorphous transition. For inspection of these tentative models, we need detailed information about intermolecular structure of C_2H_5OD in this temperature range.

4 Conclusion

Methanol and ethanol confined in ACF gave a so-called Pake doublet powder pattern characterized by the ^2H QCC of 185 kHz and the asymmetric parameter of the electric-field-gradient tensor (η) of 0.1 for both CH_3OD and C_2H_5OD. The QCC value of the deuteron was indicative of hydrogen bond formation with the O···O distance of ca. 0.27 nm. This suggested the solid-like feature of alcohols in ACFs. The quadrupole broadening vanished and the single isotropic resonance line was observed above the following temperatures: 160 K in 10A and 140 K in 20A for CH_3OD, and 200 K in 10A and 170 K in 20A for C_2H_5OD. Alcohol molecules are undergoing a rapid motion as in the bulk liquid, indicating a transition from solid to liquid in ACFs. The temperature dependence of the line width for ^2H isotropic peaks provides the average E_a values for the translation accompanying the isotropic reorientation of alcohol molecules, which were consistent with the E_a values in the bulk liquid.

The observed narrow resonance line of ^1H spectra also suggested the rapid molecular motion of alcohols in ACFs. The remarkable narrowing was also observed for the solid-like alcohols in ACFs where translation of the alcohol molecule is frozen. Therefore, the ^1H line widths are primarily modulated by the isotropic reorientation of alcohols, leading to E_a values for isotropic reorientation of the solid-like alcohols in ACFs. The E_a values in both alcohols seem to depend less on the slit width, implying a similar environment and the intermolecular interactions for alcohol molecules in ACF10A and 20A. That is, the potential barrier to molecular motion for alcohols is dominated by the special restriction due to the slit-type nanospace (hydrophobic character) as well as the intermolecular hydrogen bond (hydrophilic character). Furthermore, there were two activation processes for C_2H_5OD in 10A. The cross-over between these processes takes place at 172 K. The origin could not be identified in this study, but the feasible possibilities are proposed: One is the liquid-2D crystal transition. In this case, the cross-over will correspond to the transition from isotropic molecular reorientation to the local motion of alkyl-group. Other is the liquid-amorphous transition. In this case, the cross-over will stem from the defect formation of the hydrogen bond of C_2H_5OD confined in ACF10A.

The feasible structure of the alcohol molecules confined in ACF is examined by intermolecular interaction between the alcohol molecules and the slit walls for infinite parallel carbon sheets. The bilayer-like arrangement of the confined molecules is predicted for ACF20A with slit width of 1.1 nm. In this case, the confined molecules make it easy to form hydrogen bonds between the neighbors located along the same walls as well as along opposite walls. On the other hand, the monolayer-like structure is preferable for alcohols in ACF10A with a slit width of 0.7 nm. The restricted and anisotropic environment brings about enhancement of two-dimensionality in the intermolecular interaction.

Thus, the competition of the directionality of hydrogen bonds and a freedom of molecular orientation plays an important role in amphipathic molecules in confinement.

References

Abragam, A.: Principles of nuclear magnetism. Oxford University Press, Oxford (1961)

Berglund, B., Vaughan, R.W.: Correlations between proton chemical shift tensors, deuterium quadrupole couplings, and bond distances for hydrogen bonds in solids. J Chem Phys **73**, 2037–2043 (1980)

Eguchi, T., Soda, G., Chihara, H.: Molecular motions in polymorphic forms of ethanol as studied by nuclear magnetic resonance. Mol Phys **40**, 681–696 (1980)

Garg, S.K., Davidson, D.W.: Wide-line nuclear magnetic resonance study of solid methanols. J Chem Phys **58**, 1898–1904 (1973)

Goldammer, E.V., Hertz, H.G.: Molecular motion and structure of aqueous mixtures with nonelectrolytes as studied by nuclear magnetic relaxation methods. J Phys Chem **74**, 3734–3755 (1970)

Hurle, R.L., Easteal, A.J., Woolf, L.A.: Self-diffusion in monohydric alcohols under pressure methanol, methan(^{2}H)ol and ethanol. J Chem Soc Faraday Trans **1**(81), 769–779 (1985)

Iiyama, T., Hagi, K., Urushibara, T., Ozeki, S.: Direct determination of intermolecular structure of ethanol adsorbed in micropores using X-ray diffraction and reverse Monte Carlo analysis. Colloids Surf A **347**, 133–141 (2009)

Jönsson, P.-.G.: Hydrogen bond studies CXIII. The crystal structure of ethanol at 87 K. Acta Cryst B **32**, 232–235 (1976)

Henschel, A., Knorr, K., Huber, P.: Polymorphism of the glass former ethanol confined in mesoporous silicon. Philos Mag Lett **90**, 481–491 (2010)

Kaneko, K., Ishii, C., Ruike, M., kuwabara, H.: Origin of superhigh surface area and microcrystalline graphitic structures of activated carbons. Carbon **30**, 1075–1088 (1992)

Kaneko, K., Cracknell, R.F., Nicholson, D.: Nitrogen adsorption in slit pores at ambient temperatures: comparison of simulation and experiment. Langmuir **10**, 4606–4609 (1994)

Kaneko, K.: Molecular assembly formation in a solid nanospace. Colloids and Surf A **109**, 319–333 (1996)

Kaneko, K., Watanabe, A., Iiyama, T., Radhakrishan, R., Gubbins, K.E.: A remarkable elevation of freezing temperature of CCl_4 in graphitic micropores. J Phys Chem B **103**, 7061–7063 (1999)

Mowla, D., Do, D.D., Kaneko, K.: Adsorption of water vapor on activated carbon: a brief overview. Chem Phys Carbon **28**, 229–262 (2003)

Morishige, K.: Structure and melting of a monolayer ethanol film on graphite. J Chem Phys **97**, 2084–2089 (1992)

Nguyen, T.X., Bhatia, S.K.: How water adsorbs in hydrophobic nanospaces. J Phys Chem C **115**, 16606–16612 (2011)

Nobusawa, S., Kaku, H., Amada, T., Asano, H., Satoh, K., Ruike, M.: Calorimetric study and simulation of the adsorption of methanol and propanol onto activated carbon fibers. Colloids Surf A **419**, 100–112 (2013)

Ohba, T., Kanoh, H., Kaneko, K.: Cluster-growth-induced water adsorption in hydrophobic carbon nanopores. J Phys Chem B **108**, 14964–14969 (2004a)

Ohba, T., Kanoh, H., Kaneko, K.: Affinity transformation from hydrophilicity to hydrophobicity of water molecules on the basis of adsorption of water in graphitic nanopores. J Am Chem Soc **126**, 1560–1562 (2004b)

Ohba, T., Kanoh, H., Kaneko, K.: Water cluster growth in hydrophobic solid nanospaces. Chem Eur J **11**, 4890–4894 (2005)

Ohkubo, T., Iiyama, T., Nishikawa, K., Suzuki, T., Kaneko, K.: Pore-width-dependent ordering of C_2H_5OH molecules confined in graphitic slit nanospaces. J Phys Chem B **103**, 1859–1863 (1999a)

Ohkubo, T., Iiyama, T., Kaneko, K.: Organized structures of methanol in carbon nanospaces at 303 K studies with in situ X-ray diffraction. Chem Phys Lett **312**, 191–195 (1999b)

Ohkubo, T., Iiyama, T., Suzuki, T., Kaneko, K.: Confined state of alcohol in carbon micropores as revealed by in situ X-ray diffraction. Stud Surf Sci Catal **128**, 411–419 (2000)

Ohkubo, T., Kaneko, K.: Oriented structures of alcohol hidden in carbon micropores with ERDF analysis. Colloid Surf A **187–188**, 177–185 (2001)

Olympia, P.L., Fung, B.M.: Deuteron quadrupole coupling constants of hydrogenbonded systems. J Chem Phys **51**, 2976–2980 (1969)

Omichi, H., Ueda, T., Miyakubo, K., Eguchi, T.: Solid-state ^{2}H NMR study of nanocrystal formation of D_2O and their dynamic aspects in ACF hydrophobic nanospaces. Chem Lett **36**, 256–257 (2007)

Omichi, H., Ueda, T., Chen, Y., Miyakubo, K., Eguchi, T.: Specific molecular motion of adamantane induced by hydrophobic nano-slits in ACF as studied using solid state ^{1}H, ^{2}H and ^{13}C NMR. Mol Cryst Liquid Cryst **490**, 91–105 (2008)

Oshida, K., Kogiso, K., Matsubayashi, K., Takeuchi, K., Kobayashi, S., Endo, M., Dresselhaus, M.S., Dresselhaus, G.: Analysis of pore structure of activated carbon fibers using high resolution transmission electron microscopy and image processing. J Mater Res **10**, 2507–2517 (1995)

Pratt, K.C., Wakeham, W.A.: Self-diffusion in water and monohydric alcohols. J Chem Soc Faraday Trans **2**(73), 997–1002 (1977)

Radhakrishnan, R., Gubbins, K.E., Watanabe, A., Kaneko, K.: Freezing of simple fluids in microporous activated carbon fibers: comparison of simulation and experiment. J Chem Phys **111**, 9058–9067 (1999)

Radhakrishnan, R., Gubbins, K., Sliwinska-Bartkowiak, M.: Effect of the fluid-wall interaction on freezing of confined fluids: toward the development of a global phase diagram. J Chem Phys **112**, 11048–11057 (2000)

Radhakrishnan, R., Gubbins, K.E., Sliwinska-Bartkowiak, M.: Global phase diagrams for freezing in porous media. J Chem Phys **116**, 1147–1155 (2002a)

Radhakrishnan, R., Gubbins, K.E., Sliwinska-Bartkowiak, M.: Existence of a Hexatic Phase in Porous Media. Phys Rev Lett **89**, 076101 (2002b)

Ramos, M.A., Shmyt'ko, I.M., Arnautova, E.A., Jiménez-Riobóo, R.J., Rodríguez-Mora, V., Vieira, S., Capitán, M.J.: On the phase diagram of polymorphic ethanol: thermodynamic and structural studies. J Non-Cryst Solids **352**, 4769–4775 (2006)

Sato, M., Sukegawa, T., Suzuki, T., Kaneko, K.: Surface fractal dimension of less-crystalline carbon micropore walls. J Phys Chem B **101**, 1845–1850 (1997)

Śliwińska-Bartkowiak, M., Dudziak, G., Sikorski, R., Gras, R., Gubbins, K.E., Radhakrishnan, R.: Dielectric studies of freezing behavior in porous materials: water and methanol in activated carbon fibres. Phys Chem Chem Phys **3**, 1179–1184 (2001)

Śliwińska-Bartkowiak, M., Drozdowski, H., Kempiński, M., Jazdzewska, M., Long, Y., Palmer, J.C., Gubbins, K.E.: Structural analysis of water and carbon tetrachloride adsorbed in activated carbon fibres. Phys Chem Chem Phys **14**, 7145–7153 (2012)

Steele, W.A.: The physical interaction of gases with crystalline solids. I. Gas-solid energies and properties of isolated adsorbed atoms. Surf Sci **36**, 317–352 (1973)

Torrie, B.H., Binbrek, O.S., Strauss, M., Swainson, I.P.: Phase transitions in solid methanol. J Solid State Chem **166**, 415–420 (2002)

Ueda, T., Omichi, H., Chen, Y., Kobayashi, H., Kubota, O., Miyakubo, K., Eguchi, T.: ^{2}H NMR study of 2D melting and dynamic behaviour of $CDCl_3$ confined in ACF nanospace. Phys Chem Chem Phys **12**, 9222–9229 (2010a)

Ueda, T., Omichi, H., Chen, Y., Kobayashi, H., Kubota, O., Miyakubo, K., Eguchi, T.: Two-dimensional melting and phase change of binary mixtures of CCl_4 and $CHCl_3$ confined in ACF nano-space studied using solid-state ^1H NMR. Bull Chem Soc Jpn **83**, 1323–1332 (2010b)

Ueda, T., Omi, H., Yukioka, T., Eguchi, T.: High-pressure ^{129}Xe NMR study of the intermolecular interaction of xenon confined in activated carbon fiber (ACF). Bull Chem Soc Jpn **79**, 237–246 (2006)

Watanabe, A., Iiyama, T., Kaneko, K.: Melting temperature elevation of benzene confined in graphitic micropores. Chem Phys Lett **305**, 71–74 (1999)